Femtosecond laser lithotripsy: feasibility and ablation mechanism

Jinze Qiu
The University of Texas at Austin
Department of Biomedical Engineering
107 West Dean Keeton
Austin, Texas 78712

Joel M. H. Teichman
University of British Columbia
Department of Urologic Sciences
and
St. Paul's Hospital
1081 Burrard Street
Burrard Building C307
Vancouver, British Columbia
Canada V6Z 1Y6

Tianyi Wang
The University of Texas at Austin
Department of Biomedical Engineering
107 West Dean Keeton
Austin, Texas 78712

Joseph Neev
FemtoSec Tech Incorporated
Aliso Viejo, California

Randolph D. Glickman
The University of Texas Health Science Center
Department of Ophthalmology
San Antonio, Texas

Kin Foong Chan
Fourier Biotechnologies, LLC
San Jose, California

Thomas E. Milner
The University of Texas at Austin
Department of Biomedical Engineering
107 West Dean Keeton
Austin, Texas 78712

Abstract. Light emitted from a femtosecond laser is capable of plasma-induced ablation of various materials. We tested the feasibility of utilizing femtosecond-pulsed laser radiation (λ = 800 nm, 140 fs, 0.9 mJ/pulse) for ablation of urinary calculi. Ablation craters were observed in human calculi of greater than 90% calcium oxalate monohydrate (COM), cystine (CYST), or magnesium ammonium phosphate hexahydrate (MAPH). Largest crater volumes were achieved on CYST stones, among the most difficult stones to fragment using Holmium:YAG (Ho:YAG) lithotripsy. Diameter of debris was characterized using optical microscopy and found to be less than 20 μm, substantially smaller than that produced by long-pulsed Ho:YAG ablation. Stone retropulsion, monitored by a high-speed camera system with a spatial resolution of 15 μm, was negligible for stones with mass as small as 0.06 g. Peak shock wave pressures were less than 2 bars, measured by a polyvinylidene fluoride (PVDF) needle hydrophone. Ablation dynamics were visualized and characterized with pump-probe imaging and fast flash photography and correlated to shock wave pressures. Because femtosecond-pulsed laser ablates urinary calculi of soft and hard compositions, with micron-sized debris, negligible stone retropulsion, and small shock wave pressures, we conclude that the approach is a promising candidate technique for lithotripsy.
[DOI: 10.1117/1.3368998]

Keywords: femtosecond laser; lithotripsy; plasma; urinary calculi.

Paper 09557P received Dec. 18, 2009; accepted for publication Jan. 18, 2010; published online Apr. 14, 2010.

1 Introduction

Urinary calculi are crystal aggregations of various minerals in urine and may produce intense pain.[1] Although stones smaller than 5 mm have a good chance of spontaneous passage, stones larger than 5 mm are more likely to produce pain and obstruction, are less likely to pass, and are more likely to require surgical intervention. Laser lithotripsy is the standard treatment and uses a small-diameter flexible catheter to deliver pulsed laser light to fragment calculi.[2]

Several different lasers have been tested for clinical lithotripsy, including the flashlamp pumped pulsed dye laser (504 nm) and free-running Ho:YAG laser (2100 nm). The pulsed dye laser disintegrates stones through a photomechanical mechanism based on its short pulse duration (typically, 1 or 2 μs).[3,4] In this approach, shock waves are generated as a result of cavitation bubble expansion and collapse, disintegrating stones as they transverse calculi surfaces.[5,6] This method tends to create large-sized debris that may not pass

Address all correspondence to: Joel M. H. Teichman, University of British Columbia, Department of Urologic Sciences, 1081 Burrard Street, Burrard Building C307, Vancouver, British Columbia, V6Z 1Y6 Canada. Tel: 604-806-8266; E-mail: JTeichman@providencehealth.bc.ca

1083-3668/2010/15(2)/028001/5/$25.00 © 2010 SPIE

spontaneously through the ureter.[7] The Ho:YAG laser, with a longer pulse duration (typically 250 to 350 μs), fragments stones through a photothermal mechanism and produces smaller-sized debris than the pulsed dye laser.[7] Over the last decade, the Ho:YAG laser has become the gold standard for laser lithotripsy, as its clinical application produces small debris, it fragments all stone compositions, and Ho:YAG light is transmitted well in small-diameter optical fibers that can be positioned in a flexible ureteroscope.[8,9] Furthermore, stone-free treatment outcomes for ureteroscopy have generally exceeded 90%.[10,11] Some limitations of Ho:YAG laser lithotripsy are a relatively inefficient fragmentation (photothermal compared to photomechanical lithotripsy), increased risk of optical fiber failure, and ureteroscope destruction in lower pole ureteronephroscopy procedures.[12–14]

In an effort to identify a laser source that can fragment all stone compositions, can produce small-sized debris, and can be applied clinically, we tested an ultrashort near-infrared laser with pulse duration of 140 fs. In comparison, pulse durations employed in the current study are about one billion times shorter than those employed using Ho:YAG lithotripsy. Light emitted from a femtosecond laser is capable of plasma-induced ablation of various materials.[15] The extremely short pulse duration provided by femtosecond lasers allows substantially smaller pulsed energies for direct ionization and plasma formation. The subsequent plasma expansion fragments surrounding materials and produces small-sized debris.[16] We tested the feasibility of using femtosecond-pulsed laser radiation to ablate urinary calculi of various compositions and investigated the laser–calculi interaction mechanism.

2 Materials and Methods

2.1 *Specimens*

Human urinary calculi with compositions greater than 90% calcium oxalate monohydrate (COM), magnesium ammonium phosphate hexahydrate (MAPH), or cystine (CYST) were obtained from a stone supply laboratory (Louis Herring, Orlando, Florida). All calculi were sliced with a dental diamond saw to create a relatively flat surface before all ablation studies. The calculi were submerged in deionized water for 24 h before performing experiments.

2.2 *Experimental Setup*

The experiments were performed using a commercially available 1-W femtosecond laser (Coherent Hidra 10, Santa Clara, California) operating at a central wavelength of 800 nm and pulse duration of 140 fs. The laser was set at a pulse energy of 0.9 mJ and a beam waist diameter of 8 mm. Laser pulse repetition rate was tunable from 1 to 1000 Hz. A schematic diagram of the experimental setup is shown in Fig. 1. A shutter (UniBlitz Model LS6Z, Vincent Associates, Rochester, New York) was positioned after the laser exit aperture and operated by a shutter controller (UniBlitz Model T132, Vincent Associates). A 30× objective lens (NA=0.40) with a 3.8-mm working distance was used to focus laser radiation on the calculus specimen. The aberration-free beam diameter at the objective lens focus was calculated to be 2.4 μm. Single-pulse energy just before interacting with the calculus sample

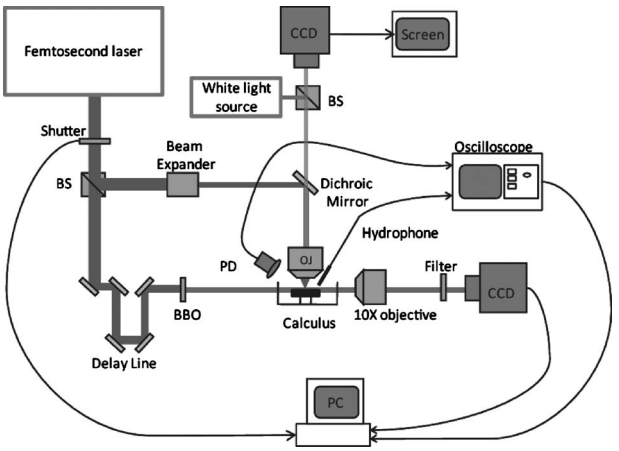

Fig. 1 Experimental setup to investigate femtosecond laser ablation of urinary calculi.

was measured to be 0.64 mJ. Power density on the test specimen during the pulse was estimated at 10^{17} W/cm^2, substantially higher than the threshold to produce plasma-mediated ablation in most materials.[15] Each calculus sample was submerged in water (3.8 mm below air–water interface) and irradiated with 1000 pulses at a pulse repetition rate of 1 KHz. Six specimens of each composition (COM, MAPH, CYST) were irradiated. A flat area of calculus was irradiated and longitudinal position of the stone surface was maintained 50 μm above the minimum beam waist in water (n=1.32). A dichroic mirror that reflected near-infrared femtosecond light and transmitted visible light was utilized to allow the CCD camera to share the same objective lens with the ablation optical path for image monitoring. After femtosecond-pulsed laser irradiation, calculi and debris were desiccated in air. Crater diameter and depth were measured using spectral domain optical coherence tomography (OCT).[4] The elementary volume equation for a cone (1/3·base·height) was used to estimate crater volume. Size of ejected debris was characterized by optical microscopy.

The light source for the pump-probe imaging experiments was the same Hidra 10 femtosecond laser used for ablation studies (Fig. 1). The pump and probe beams were generated using a 75:25 beamsplitter, respectively. The reduced energy beam used for probing was frequency doubled with a 4-mm-thick beta-barium borate (BBO) crystal. A variable optical delay line was included in the probe beam path to achieve specific time delays (0 to 59 ns) between pump and probe pulses. A highspeed camera (FASTCAM Super 3K, Photron, San Diego, California) was synchronized with the shutter controller to record time-resolved images of debris ejection after the calculus was ablated with a single pulse. For each pump-probe image, the calculus was moved to a new lateral position with a virgin surface before a second image was recorded. A 450-nm shortpass optical filter (FES0450 Thorlabs, Newton, New Jersey) was positioned in front of the camera to block residual 800-nm light and fluorescence light generated during ablation. The 30× objective lens for ablation was replaced by a 16× objective lens (working distance 8 mm; NA 0.25) to provide a longer working distance for pump-probe imaging.

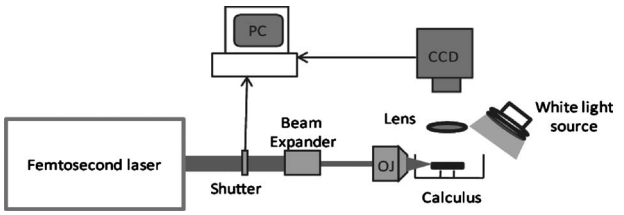

Fig. 2 Experimental setup to investigate dynamics of stone retropulsion.

Fast flash photography was used to record images of the ablation site at pump-probe delays from fractions of a microsecond to tens of microseconds. The setup employed for fast flash photography was similar to that utilized for pump probe imaging except for the probe light source and the filter. A microchip laser (Standa STA-01-10, Vilnius, Lithuania, wavelength 1064 nm, pulse duration 0.4 ns, pulse energy 12.5 μJ) was used as a probe light source. The 450-nm filter was replaced by a 950-nm longpass filter (FEL0950 Thorlabs, Newton, New Jersey) to allow transmission of only radiation emitted by the microchip laser. The delay between onset of the femtosecond laser pump pulse and the microchip laser probe pulse was controlled by a digital delay generator (DG535, Standard Research Systems, Sunnyvale, California). A series of delay times (0.65 to 73.5 μs) was used to record fast flash photographs of ablation events.

The shock wave pressure produced by superheating of calculi and plasma expansion was measured by a polyvinylidene fluoride (PVDF) needle hydrophone (TNU001A, NTR Systems, Seattle). The PVDF hydrophone had a linear response from 0.002 MHz to 50 MHz and could detect most shock waves created by femtosecond laser ablation. The acoustic signals were amplified by an NTR 30-dB preamplifier (10 to 90% rise time is 7 ns) and acquired via a digital oscilloscope. During ablation, a fraction of incident femtosecond laser light was reflected by the calculus surface and was collected by a fast Si photoreceiver (1801-FS, New Focus, San Jose, California; 125 MHz) to trigger acquisition of the shock wave pressure measurement.

The dynamics of stone retropulsion during ablation were monitored using a second experimental setup (Fig. 2). Femtosecond laser pulses were incident on and interacted with calculi specimens from the side. A calculus sample was placed on a smooth glass surface to minimize the static frictional force between the stone and supporting interface. A high-speed camera (FASTCAM Super 3K, Photron, San Diego, California) was synchronized with the shutter to record time-resolved images and detect any retropulsive movement of the calculus sample. The spatial resolution of recorded images was calibrated to be 15 μm.

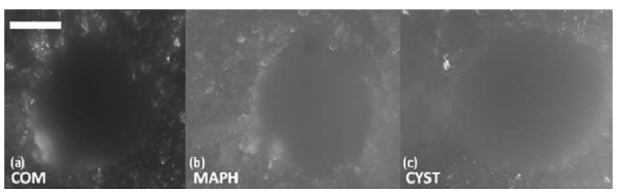

Fig. 3 Microscopic images of ablation craters on COM (a), CYST (b), and MAPH (c) calculi.

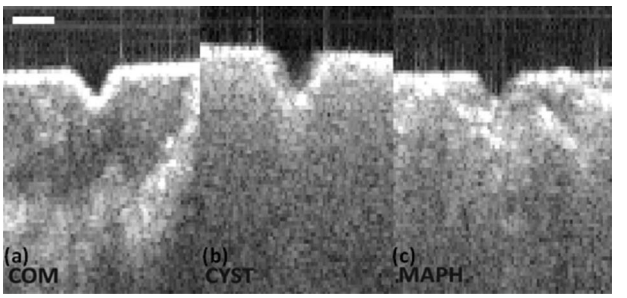

Fig. 4 OCT cross-sectional images of ablation craters on (a) COM, (b) CYST, and (c) MAPH calculi.

3 Results

Conically shaped ablation craters were produced in COM, CYST, and MAPH calculi (Figs. 3 and 4) as a result of femtosecond-pulsed laser irradiation. Edges of all craters were sharp and clearly observed in the microscopic and OCT images. The crater diameters and depths varied from tens of microns to several hundred microns (Fig. 5). Crater volumes for CYST calculi were twice as large as that for COM and MAPH. The size of most debris was below 1 μm for COM, CYST, and MAPH calculi compositions. Debris with size ranging from 1 μm to 20 μm were observed in much smaller proportions. No debris larger than 20 μm in diameter were observed .

Femtosecond bubble dynamics are shown in Fig. 6 (0 to 59 ns: pump-probe imaging; 0.65 to 32.3 μs: fast flash photography). For reference in all measurements, the femtosecond laser pulse interacted with the calculus surface at $t=0$ ns. A conical-shaped plasma feature formed in water before a 7-ns delay, indicating that radiation energy density exceeded the plasma threshold in regions outside the minimum beam waist. At a 7-ns delay, a shock wave separated from the plasma and propagated outward. Although the plasma region did not expand substantially over the initial 59 ns after the pump pulse, expansion was observed at a microsecond time scale. The fastest expansion was observed at the tip of the cone, where energy density was highest. Maximum expansion

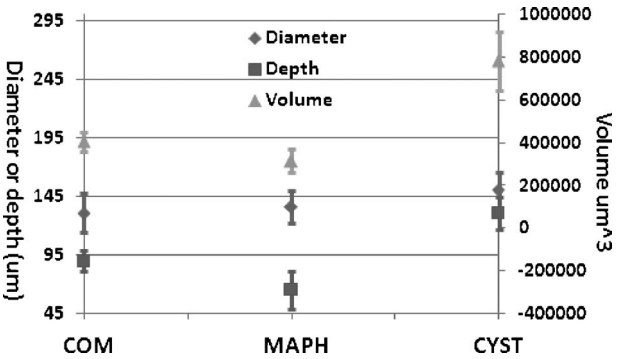

Fig. 5 Diameter, depth, and volume of ablation craters in COM, MAPH, and CYST calculi.

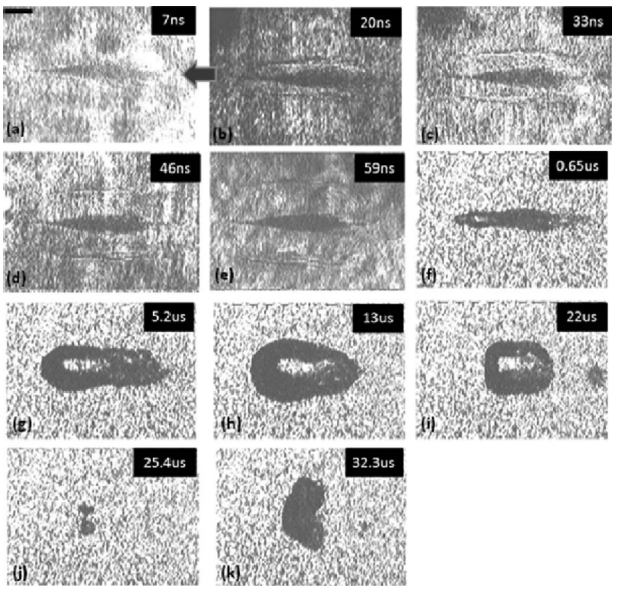

Fig. 6 Images of femtosecond bubble dynamics in water.

was recorded at 13 μs, and a pear-shaped vapor bubble was observed. Thereafter, the bubble began to collapse and formed the shape of a cylinder. The bubble reached a minimum volume at 25 μs and began a second cycle of expansion afterward.

Images of femtosecond-pulsed laser ablation dynamics were recorded (Fig. 7) at various delay times using pump-probe imaging (0 to 59 ns) and fast flash photography

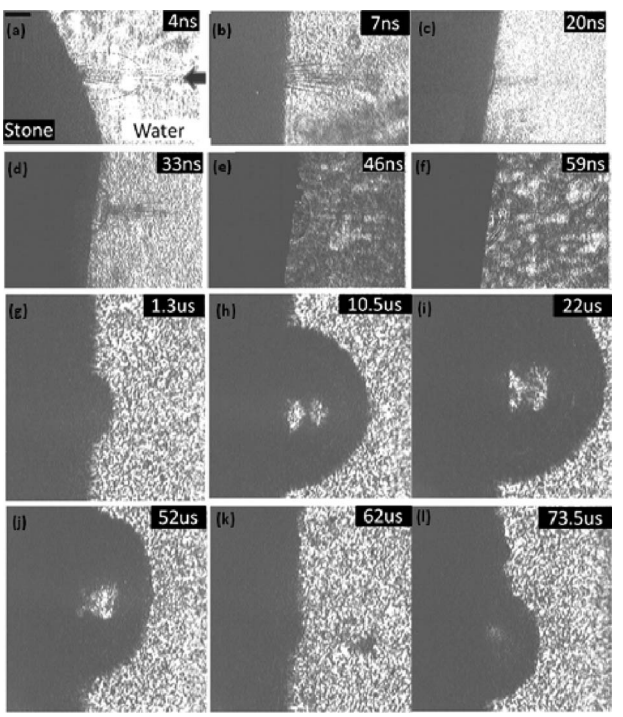

Fig. 7 Images of femtosecond ablation dynamics. Cystine was used to demonstrate, but no obvious difference is observed for different calculi.

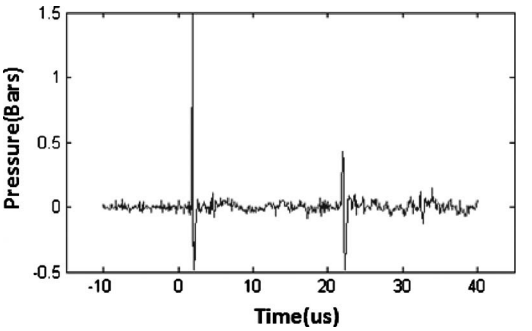

Fig. 8 Shock wave pressures measured during femtosecond laser ablation in pure water.

(1.3 to 73.5 μs). A portion of the femtosecond pump pulse laser energy created localized microplasmas in water within the initial 4 ns and formed a pattern tracing propagation of the beam. The localized microplasmas did not substantially alter the beam propagation[15] in water so that a large portion of the incident radiant energy passed through and was sufficient to create plasma on the surface of the calculus sample. Due to rapid plasma expansion on the calculus surface, a hemispherical shock wave was observed to separate and propagate outward from the plasma within 20 ns of the onset of the femtosecond pump pulse. A hemispheric bubble first became evident at a delay time of 33 ns and continued expanding by following shock wave propagation. The bubble reached a maximum size at 22 μs. Thereafter, the bubble began to collapse and reached a minimum volume at 62 μs and subsequently began a second cycle of expansion. Debris were visible in the image recorded at 62 μs. The speed of shock wave expansion was calculated based on pump-probe images and was approximately 2.1 μm/ns at 7 ns delay, or 1.4 times the speed of sound in water, and decreased to 1.5 μm/ns at 20-ns delay, nearly equal to the speed of sound in water.

Shock wave pressures measured for water ablation are displayed in Fig. 8. Two pressure peaks were observed when the PVDF hydrophone was placed within several hundred microns from the ablated region. The first peak pressure (1.5 bars) corresponded to the shock wave separating from the plasma (t=20 ns; Fig. 6). The second peak (0.4 bar) corresponded to secondary expansion of the vapor bubble (t =25.4 μs; Fig. 6).

No retropulsion movement was detected within the spatial resolution of the camera (15 μm) for all three calculi compositions when maximum femtosecond-pulsed laser energy (0.64 mJ) was applied to small calculi specimens (0.06 g).

4 Discussion

The ablation process of femtosecond laser lithotripsy in these experiments is governed by a plasma-mediated ablation mechanism and appears fundamentally distinct from that of nanosecond laser lithotripsy. Nanosecond laser lithotripsy is governed by a photomechanical ablative mechanism.[5,6,17] In nanosecond laser lithotripsy, shock waves are generated by both plasma expansion and bubble collapse with a magnitude of over 100 bars[2]. These shock waves are powerful enough to fragment calculi when they traverse the calculus surface. In

the femtosecond laser lithotripsy experiments reported here, the calculus is ionized at the beginning of the femtosecond laser pulse and forms a plasma (mixture of ions and electrons). Following ionization and plasma creation, incoming laser energy is absorbed by free electrons, providing acceleration and additional free electron creation.[18] The number of high-speed free electrons is sufficiently large to remove calculus material. The plasma-mediated ablation mechanism is consistent with the observation of small-sized debris. All debris were less than 20 μm in diameter, and most debris were less than 1 μm in diameter. In comparison, nanosecond laser lithotripsy produces large debris with sizes from several hundred microns to several millimeters.[5–7,17] Larger debris are more likely to obstruct the ureter.[1]

Because the energy transfer time from plasma electrons to ions by collisions is on the order of several picoseconds (1 ps=1000 fs) and is much longer than the laser pulse duration (140 fs),[18] only a small fraction of incident laser energy was transferred to heat the ions and produce shock waves. Amplitude of shock wave pressures is thus smaller than those observed in nanosecond laser lithotripsy and consistent with experimental values (1.5 bars and 0.4 bar) reported here. Large-amplitude shock waves produce irregular fracture planes,[6] whereas plasma-induced ablation craters observed in our experiments appeared more smooth and symmetric. In nanosecond laser lithotripsy, shock wave speed decreases to a value close to speed of sound in water within a distance of about 200 μm from the emission center.[19] In comparison, shock waves produced in femtosecond laser lithotripsy slow to the speed of sound in water within a distance less than 100 μm. The rapid decay of the shock wave speed suggests that the shock wave does not substantially contribute to the femtosecond ablation process.

In our experiments, femtosecond laser ablation of calculi shows several interesting features that may provide advantages for laser lithotripsy. First, femtosecond laser lithotripsy produces micron-sized debris. The small debris size compares favorably to Ho:YAG lithotripsy.[7] Second, the paucity of shock waves and reduced amplitude implies little risk of retropulsion or collateral damage.[4] Absence of retropulsion during laser lithotripsy is desirable.[4,20] Third, the ultrashort pulse duration implies little risk of heat accumulation or thermal transfer, with little risk of collateral thermal damage.[21]

Observations from these preliminary studies suggest that further investigation of femtosecond laser lithotripsy is warranted. In the experiments reported here, we delivered femtosecond laser pulses to calculi specimens as a focused free beam. Clinical laser lithotripsy will require use of a waveguide to deliver femtosecond light to a targeted calculi.[22] Future studies in our laboratory investigating use of femtosecond laser light for clinical laser lithotripsy are planned and will be reported.

Acknowledgments

The author would like to thank Roman Kuranov, PhD, for assistance with OCT imaging. We gratefully acknowledge the stone reference laboratory (Louis Herring, Orlando, Florida) for providing human calculi specimens used for this study.

References

1. J. M. H. Teichman, "Clinical practice: acute renal colic from ureteral calculus," *New Eng. J. Med.* **350**(7), 684–693 (2004).
2. S. Brewster, D. Cranston, and J. Noble, *Urology: A Handbook for Medical Students* pp. 81–89, Informa Health Care, Oxford, UK (2001).
3. K. F. Chan, B. Choi, G. Vargas, D. X. Hammer, B. Sorg, T. J. Pfefer, J. M. H. Teichman, A. J. Welch, and E. D. Jansen, "Free electron laser ablation of urinary calculi: an experimental study," *IEEE J. Sel. Top. Quantum Electron.* **7**(6), 1022–1033 (2001).
4. H. W. Kang, H. Lee, J. M. H. Teichman, J. O. Oh, J. Kim, and A. J. Welch, "Dependence of calculus retropulsion on pulse duration during Ho:YAG laser lithotripsy," *Lasers Surg. Med.* **38**(8), 762–772 (2006).
5. K. Rink, G. Delacretaz, and R. P. Salathe, "Fragmentation process of current laser lithotriptors," *Lasers Surg. Med.* **16**(2), 134–146 (1995).
6. K. F. Chan, H. Lee, J. M. H. Teichman, A. Kamerer, H. S. McGuff, G. Vargas, and A. J. Welch, "Erbium:YAG laser lithotripsy mechanism," *J. Urol. (Baltimore)* **168**(2), 436–441 (2002).
7. J. M. Teichman, G. J. Vassar, J. T. Bishoff, and G. C. Bellman, "Holmium:YAG lithotripsy yields smaller fragments than lithoclast, pulsed dye laser or electrohydraulic lithotripsy," *J. Urol. (Baltimore)* **159**(1), 17–23 (1998).
8. G. J. Vassar, J. M. H. Teichman, and R. D. Glickman, "Holmium:YAG lithotripsy efficiency varies with energy density," *J. Urol. (Baltimore)* **160**(2), 471–476 (1998).
9. J. M. Teichman, G. J. Vassar, and R. D. Glickman, "Holmium:yttrium-aluminum-garnet lithotripsy efficiency varies with stone composition," *Urology* **52**(3), 392–397 (1998).
10. M. Sofer, J. D. Watterson, T. A. Wollin, L. Nott, H. Razvi, and J. D. Denstedt, "Holmium:YAG laser lithotripsy for upper urinary tract calculi in 598 patients," *J. Urol. (Baltimore)* **167**(1), 31–34 (2002).
11. J. M. H. Teichman, R. D. Rao, V. J. Rogenes, and J. M. Harris, "Ureteroscopic management of ureteral calculi: electrohydraulic versus holmium:YAG lithotripsy," *J. Urol. (Baltimore)* **158**(4), 1357–1361 (1997).
12. N. S. Corbin, J. M. Teichman, T. Nguyen, R. D. Glickman, L. Rihbany, M. S. Pearle, and J. T. Bishoff, "Laser lithotripsy and cyanide," *J. Endourol* **14**(2), 169–173 (2000).
13. B. E. Knudsen, R. D. Glickman, K. J. Stallman, S. Maswadi, B. H. Chew, D. T. Beiko, J. D. Denstedt, and J. M. H. Teichman, "Performance and safety of holmium: YAG laser optical fibers," *J. Endourol* **19**(9), 1092–1097 (2005).
14. A. C. Mues, J. M. H. Teichman, and B. E. Knudsen, "Evaluation of 24 holmium:YAG laser optical fibers for flexible ureteroscopy," *J. Endourol* **182**(1), 348–354 (2009).
15. R. R. Gattass and E. Mazur, "Femtosecond laser micromachining in transparent materials," *Nature Photon.* **2**, 219–225 (2008).
16. A. V. Kabashin and M. Meunier, "Synthesis of colloidal nanoparticles during femtosecond laser ablation of gold in water," *J. Appl. Phys.* **94**(12), 7941–7943 (2003).
17. K. Rink, G. Delacretaz, and R. P. Salathe, "Fragmentation process induced by nanosecond laser pulses," *Appl. Phys. Lett.* **61**(22), 2644–2646 (1992).
18. E. G. Gamaly, A. V. Rode, B. Luther-Davies, and V. T. T.Tikhonchuk, "Ablation of solids by femtosecond lasers: ablation mechanism and ablation thresholds for metals and dielectrics," *Phys. Plasmas* **9**(3), 949–957 (2002).
19. A. Vogel, S. Busch, and U. Parlitz, "Shock wave emission and cavitation bubble generation by picosecond and nanosecond optical breakdown in water," *J. Acoust. Soc. Am.* **100**(1), 148–165 (1996).
20. D. S. Finley, J. Petersen, C. Abdelshehid, M. Ahlering, D. Chou, J. Borin, L. Eichel, E. McDougall, and R. Clayman, "Effect of holmium:YAG laser pulse width on lithotripsy retropulsion *in vitro*," *J. Endourol* **19**(8), 1041–1044 (2005).
21. K. F. Chan, T. J. Pfefer, J. M. Teichman, and A. J. Welch, "A perspective on laser lithotripsy: the fragmentation processes," *J. Endourol* **15**(3), 257–273 (2001).
22. O. A. Nazif, J. M. H. Teichman, R. D. Glickman, and A. J. Welch, "Review of laser fibers: a practical guide for urologists," *J. Endourol* **18**(9), 818–829 (2004).